Inorganic Chemistry
Article
pubs.acs.org/IC

Synthesis, Structure, and Reactivity of Iridium(III) Complexes Containing a 4,6-Dimethyl-1,3-benzenediphenylimine Pincer Ligand

Leah A. Wingard,* Mathew C. Finniss, Michael Norris, Peter S. White, Maurice Brookhart, and Joseph L. Templeton

W. R. Kenan Laboratory, Department of Chemistry, University of North Carolina, Chapel Hill, North Carolina 27599-3290, United States

Ⓢ *Supporting Information*

ABSTRACT: A nonheterocyclic bis(imino)aryl ligand with blocking methyl substituents, 4,6-dimethyl-1,3-benzenediphenylimine (NCHN), has been synthesized. Metalation via oxidative addition proceeds under mild conditions with the Ir(I) reagent $[Ir(CH_2{=}CH_2)_2(Cl)]_2$ to produce the Ir(III) product $(NCN)Ir(CH_2CH_3)(Cl)$. Neutral nucleophiles such as water or triphenylphosphine add readily to the vacant sixth coordination site. Protonation of the ethyl group results in loss of ethane and formation of a dicationic chloride-bridged (NCN)Ir dimer. Alternatively, the chloride ligand can be abstracted from $(NCN)Ir(CH_2CH_3)(Cl)$ to provide access to various neutral and cationic species, including $(NCN)Ir(CH_2CH_3)(OAc)$ (OAc = acetate), $[(NCN)Ir(CH_2CH_3)(bpy)][BF_4]$ (bpy = 4,4′-bipyridine), $[(NCN)Ir(CH_2CH_3)(NCCH_3)_2][BF_4]$, and $[(NCN)Ir(CH_2CH_3)(OH_2)_2][BF_4]$, which is water soluble.

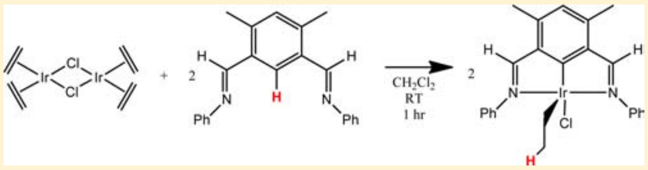

INTRODUCTION

Designing new ligands with desirable properties is one of the most important goals in organometallic chemistry. Altering ligand frameworks allows for systematic variation of the chemical properties of metal complexes in a controlled and predictable manner. Pincer ligands, which are defined by tridentate meridional coordination to a metal center in accord with the picturesque name, have been known since the 1970s.[1−6] Because of the ease with which synthetic variations of pincer substituents can be accomplished and the ability of pincer ligands to stabilize mononuclear complexes, the use of pincer ligands has rapidly expanded across organometallic chemistry.[7,8] Pincer complexes have found widespread use as catalysts in transition metal mediated processes such as C−C bond forming reactions, polymerizations, transfer hydrogenation, and dehydrogenation reactions.[9,10] Pincer complexes can also be used as sensors,[11−13] and they are particularly helpful in initiating C−C, C−H, and C−O bond activation processes.[14]

The typical tridentate meridional coordination mode of a pincer with a central aryl ring forces the aryl ring into a conformation nearly coplanar with the coordination plane of d^8 square-planar metal centers or with the basal plane of d^6 square-pyramidal metal centers.[9] Pincer ligands have been successfully coordinated to all of the group VIIIB transition metals, and the resulting complexes have been used for numerous purposes. Iridium pincer complexes exhibit a wide range of reactivity, with applications which include electrocatalytic reduction of CO_2,[15,16] C−H bond cleavage,[17−21] alkane metathesis,[22,23] and various dehydrogenation reactions.[8,24−37] The pincers used have typically been PCP[16,21,37] or POCOP[38,39]-type ligands. When occupying the central site of the tridentate pincer ligand, the M-C bond exhibits excellent thermal stability.

Changing to nitrogen donors from phosphorus donors may increase ligand stability under oxidative conditions. Bis(imino)-aryl pincer metal complexes have increased in popularity over the past decade.[40−44] Known Ir(III) complexes include pincer ligands with heterocyclic N-donor moieties including pyridyl,[45,46] benzimidazolyl,[47,48] and oxazolyl[49] groups. Nonheterocyclic bis(imino)aryl iridium complexes are less common,[50] and synthetic routes are limited. Metalation of nonheterocyclic bis(imino)aryl ligands at the aryl 2- position can be challenging because C−H activation at the 4- or 6-position resulting in bidentate binding is kinetically favored (Scheme 1). Since only C−H activation at the 2- position results in tridentate ligand binding, yields of κ^3 complexes are often low. Synthetically, blocking both the 4- and the 6- sites with substituents has resulted in more favorable metalation of the central 2- site.[49] These NCN-type pincer complexes of iridium have been shown to have catalytic hydrogen-transfer abilities,[50] applications to asymmetric synthesis,[49] and luminescent and emissive properties.[45−48] Herein we present the synthesis of a bis(imino)aryl NCHN ligand with methyl groups at the 4- and 6- sites, and metalation of this ligand by iridium under mild conditions.

RESULTS AND DISCUSSION

Ligand Design and Synthesis. Pursuing a simple nonheterocyclic bis(imino)aryl ligand for facile coordination to Ir(III), we synthesized 4,6-dimethyl-1,3-benzenediphenyli-

Received: November 27, 2012
Published: December 24, 2012

dx.doi.org/10.1021/ic302589b | *Inorg. Chem.* 2013, 52, 515−526

Scheme 1. Bidentate Coordination of Non-Heterocyclic Bis(imino)aryl Ligands

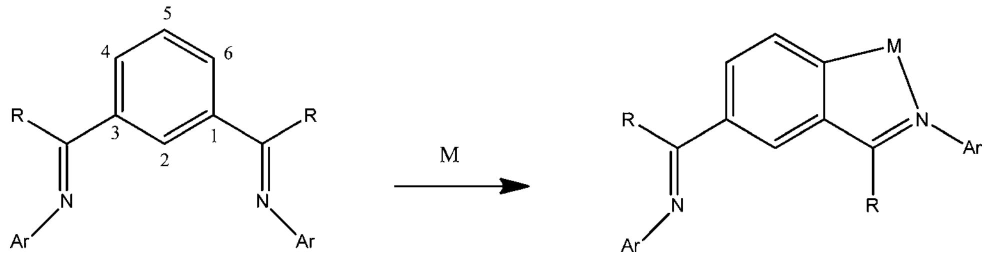

Scheme 2. Synthetic Route to 4,6-Dimethyl-1,3-bis(phenylimino)benzene

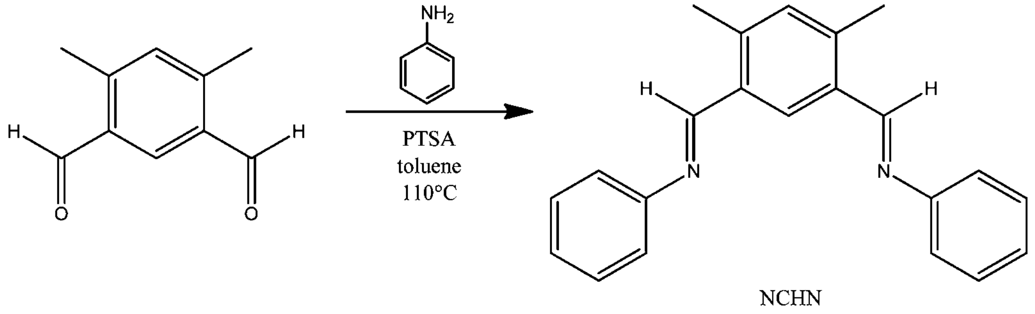

Scheme 3. Synthetic Route to (NCN)Ir(CH_2CH_3)(Cl) (2)

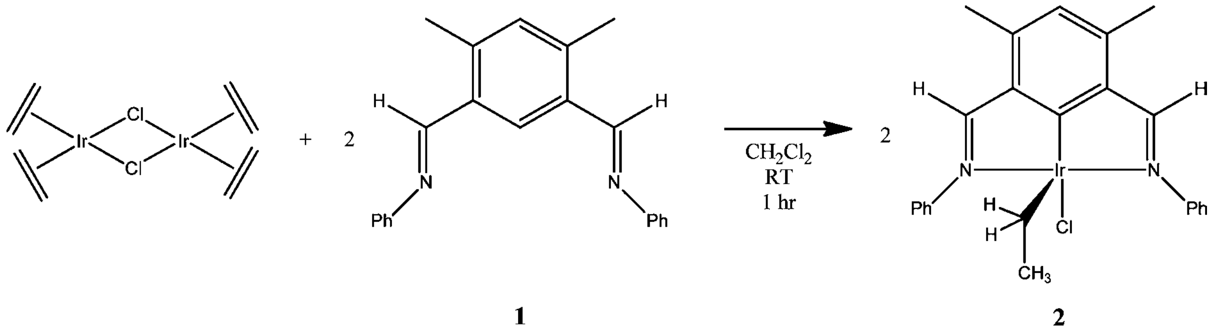

Scheme 4. Synthetic Route to (NCN)Ir(CH_2CH_3)(Cl)(OH_2) (3)

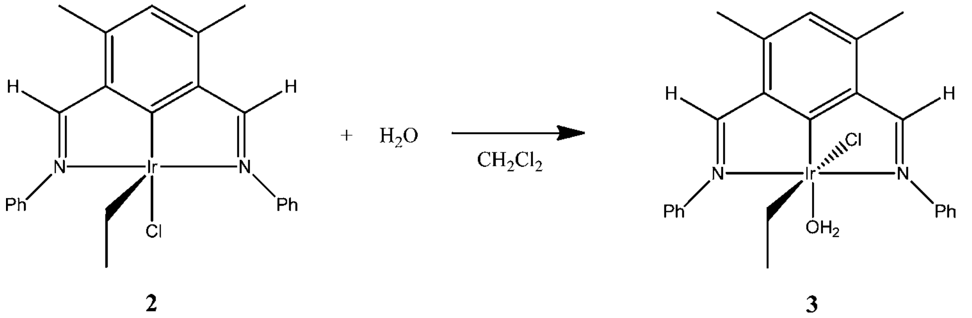

mine. As previously shown, C−H activation at the 4- and 6- positions of the aryl ring is favored over the desired C−H activation at the 2- position, resulting in formation of bidentate CN chelates rather than the desired tridentate NCN complexes (Scheme 1). To guide C−H activation to the 2- position, methyl groups were placed in the 4- and 6- positions. The methyl groups provide the additional benefit of serving as convenient NMR handles for both proton and carbon spectra.

4,6-Dimethyl-1,3-benzenedicarboxaldehyde was synthesized according to literature procedures.[51−53] The dialdehyde reacts with 2 equiv of aniline and a catalytic amount of *p*-toluenesulfonic acid (PTSA) in refluxing toluene to produce the electron-rich bis(imino)aryl ligand, 4,6-dimethyl-1,3-benzenediphenylimine (**1**, NCHN) (Scheme 2). The diimine product is isolated by removal of toluene followed by washing the residue with methanol to produce an air-stable off-white powder.

The ^1H NMR spectrum of 4,6-dimethyl-1,3-bis-(phenylimino)benzene (NCHN) shows C_{2v} symmetry with a downfield signal at 8.75 ppm representing the two equivalent imino protons. The central aryl proton *ortho* to both imino groups appears as a singlet at 8.66 ppm. The imino phenyl rings

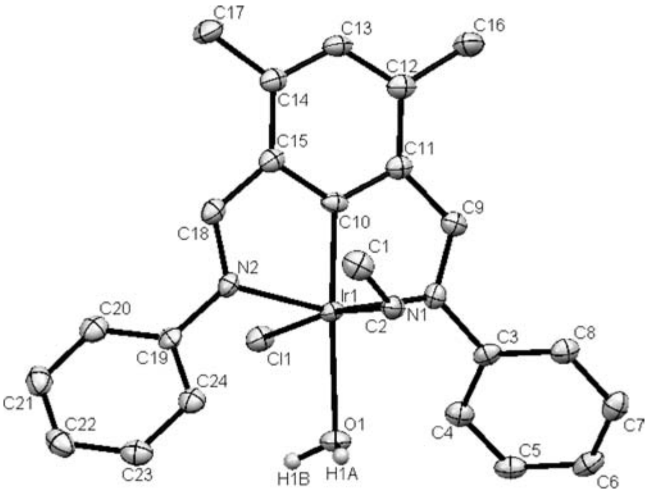

Figure 1. ORTEP diagram of $(NCN)Ir(CH_2CH_3)(Cl)(OH_2)$ (**3**).

Table 1. Bond Lengths and Bond Angles of 3

bond distances (Å)		bond angles (deg)	
Ir(1)−Cl(1)	2.4831(8)	N(1)−Ir(1)−N(2)	159.35(12)
Ir(1)−O(1)	2.259(2)	N(1)−Ir(1)−C(10)	79.75(13)
Ir(1)−N(1)	2.051(3)	N(2)−Ir(1)−C(10)	79.64(13)
Ir(1)−N(2)	2.056(3)	C(10)−Ir(1)−Cl(1)	99.05(10)
Ir(1)−C(2)	2.095(3)	C(10)−Ir(1)−O(1)	176.88(12)
Ir(1)−C(10)	1.901(3)	C(10)−Ir(1)−C(2)	90.02(13)
		C(2)−Ir(1)−Cl(1)	170.92(10)
		C(2)−Ir(1)−O(1)	88.50(11)
		O(1)−Ir(1)−Cl(1)	82.43(7)

are symmetric and exhibit a doublet at 7.42 ppm for the four protons in the *ortho* positions, a triplet at 7.24 ppm for the two protons in the *para* positions, and a triplet at 7.26 ppm for the four protons in the *meta* positions. The aryl proton at the 5-position *ortho* to both methyl groups of the central ring appears at 7.15 ppm. A singlet at 2.65 integrating for six protons is observed for the equivalent methyl groups.

Metalation of the NCHN Pincer Ligand. Attempts to metalate the NCHN ligand with traditional iridium sources, such as $IrCl_3 \cdot 3H_2O$, $[Ir(COE)_2(Cl)]_2$ (COE = cyclooctene), and $[Ir(COD)(Cl)]_2$ (COD = 1,5-cyclooctadiene), result in complex reaction mixtures regardless of reaction time or temperature. The chloride-bridged Ir(I) ethylene dimer[54] proved to be an ideal iridium source for adding the NCHN ligand. Addition of 2 equiv of the NCHN ligand to a methylene chloride solution of $[Ir(CH_2{=}CH_2)_2(Cl)]_2$ at room temperature followed by stirring for 1 h results in clean metalation of the NCN ligand by activation of the central aryl C−H bond, giving $(NCN)Ir(CH_2CH_3)(Cl)$ (**2**) (Scheme 3). Complex **2** is isolated in good yield as a red powder by removal of methylene chloride and washing with pentane.

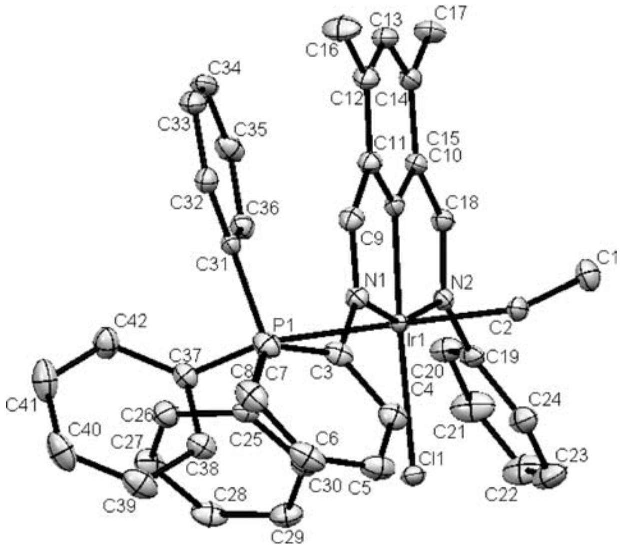

Figure 2. ORTEP of $(NCN)Ir(CH_2CH_3)(Cl)(PPh_3)$ (**4**).

Table 2. Bond Lengths and Bond Angles of 4

bond distances (Å)		bond angles (deg)	
Ir(1)−Cl(1)	2.5062(6)	N(1)−Ir(1)−N(2)	157.76(8)
Ir(1)−P(1)	2.3800(6)	N(1)−Ir(1)−C(10)	79.00(9)
Ir(1)−N(1)	2.0818(19)	N(2)−Ir(1)−C(10)	78.83(9)
Ir(1)−N(2)	2.0869(19)	C(10)−Ir(1)−Cl(1)	176.48(7)
Ir(1)−C(2)	2.136(2)	C(10)−Ir(1)−P(1)	94.54(7)
Ir(1)−C(10)	1.922(3)	C(10)−Ir(1)−C(2)	86.58(9)
		C(2)−Ir(1)−Cl(1)	90.00(7)
		C(2)−Ir(1)−P(1)	177.56(7)
		P(1)−Ir(1)−Cl(1)	88.844(19)

The metalation of **1** was monitored by NMR spectroscopy at low temperature. Upon addition of 2 equiv of ligand **1** to a CD_2Cl_2 solution of $[Ir(CH_2{=}CH_2)_2(Cl)]_2$ at 215 K (a 1:1 ratio of ligand to metal), the ^1H NMR spectrum shows that the two halves of the ligand are inequivalent; the imino protons and the methyl groups of the NCHN ligand are no longer equivalent. The central aryl proton between the two imino groups shifts far downfield to 11.2 ppm. Additionally, free ethylene appears in the spectrum. We postulate that one

Scheme 5. Synthetic Route to $(NCN)Ir(CH_2CH_3)(Cl)(PPh_3)$ (4)

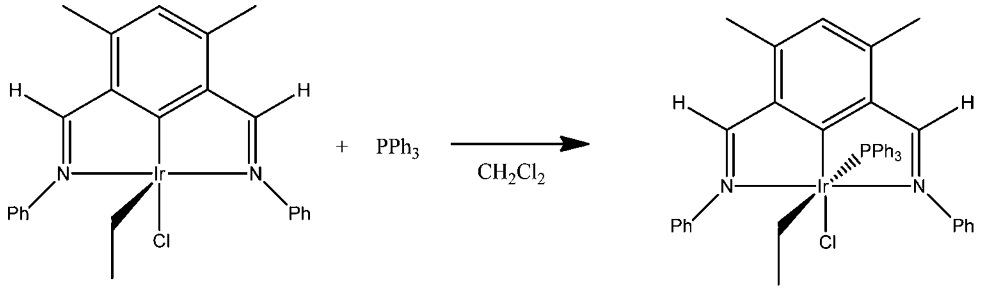

Scheme 6. Synthetic Route to $[(NCN)IrCl]_2[OTf]_2$ (5)

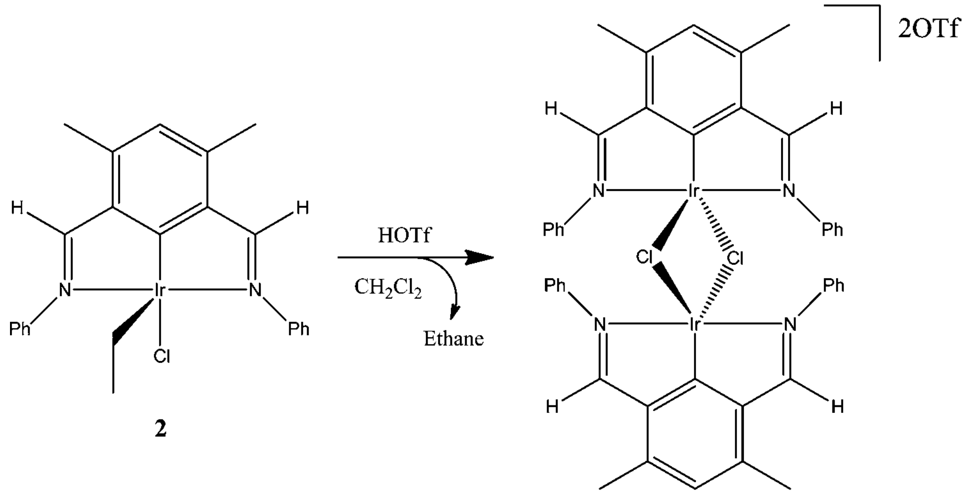

2

5

Scheme 7. Synthetic Route to $(NCN)Ir(CH_2CH_3)(OAc)$ (6)

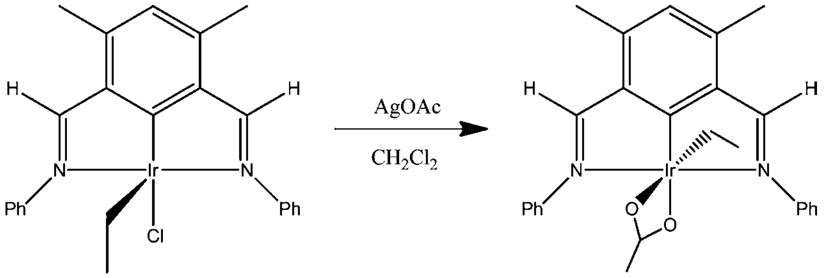

2

6

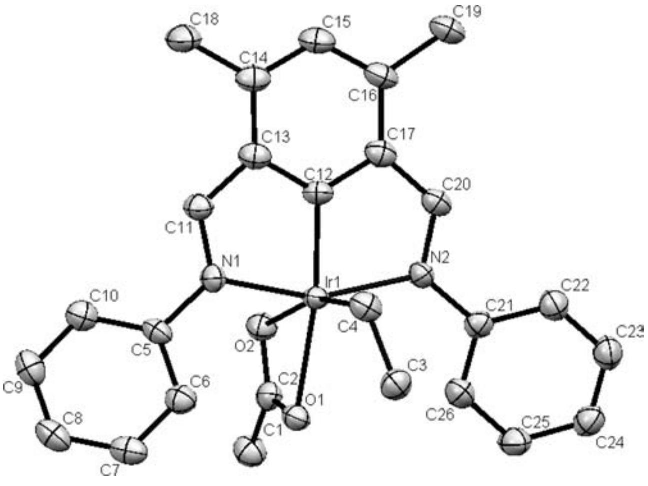

Figure 3. ORTEP of $(NCN)Ir(CH_2CH_3)(OAc)$ (**6**).

Table 3. Bond Lengths and Bond Angles of $(NCN)Ir(CH_2CH_3)(OAc)$ (6)

bond distances (Å)		bond angles (deg)	
Ir(1)−O(1)	2.281(3)	N(1)−Ir(1)−N(2)	158.64(15)
Ir(1)−O(2)	2.248(3)	N(1)−Ir(1)−C(12)	79.31(16)
Ir(1)−N(1)	2.067(3)	N(2)−Ir(1)−C(12)	79.33(15)
Ir(1)−N(2)	2.096(3)	C(12)−Ir(1)−O(1)	166.09(14)
Ir(1)−C(4)	2.070(4)	C(12)−Ir(1)−O(2)	108.36(14)
Ir(1)−C(12)	1.899(4)	C(12)−Ir(1)−C(4)	89.56(16)
		C(4)−Ir(1)−O(1)	104.19(13)
Ir(1)−C(2)	2.627(4)	C(4)−Ir(1)−O(2)	162.05(14)
		O(1)−Ir(1)−O(2)	57.86(10)

ethylene ligand is displaced from each iridium center by one imino group, resulting in formation of an intermediate chloride-bridged iridium(I) dimer with one η^2-ethylene and a monodentate nitrogen-bound NCHN ligand in the coordination sphere of each iridium. Although no other additional intermediates are observed by NMR spectroscopy, some sequence of coordination of the second imino group, dimer dissociation, and C−H activation would result in an $(NCN)Ir(CH_2CH_2)(H)(Cl)$ intermediate that could then insert ethylene into the Ir−H bond to form the observed metal complex $(NCN)Ir(CH_2CH_3)(Cl)$, **2**. Note that β-H elimination from **2** is not observed even upon heating the complex.

The ^1H NMR spectrum of **2** shows a C_s symmetric iridium(III) complex. The imino protons are equivalent and appear as a singlet at 8.82 ppm. The signal for the remaining proton on the central aryl ring shifts upfield to 6.8 ppm, the two methyl groups are equivalent at 2.66 ppm, and the metal-bound ethyl group exhibits a quartet at 0.96 ppm and a triplet at −0.16 ppm. The ^{13}C NMR spectrum is consistent with the proton spectrum. The resonance for the equivalent imino carbons appears at 175.1 ppm while the phenyl and aryl carbons fall between 152 and 123 ppm. The equivalent methyl carbons resonate at 19.7 ppm. The signals of $-CH_2-$ and $-CH_3$ of the ethyl group appear at 15.2 ppm and −12.9 ppm, respectively,

Scheme 8. Synthetic Route to $[(NCN)Ir(CH_2CH_3)(NCCH_3)_2][BF_4]$ (7)

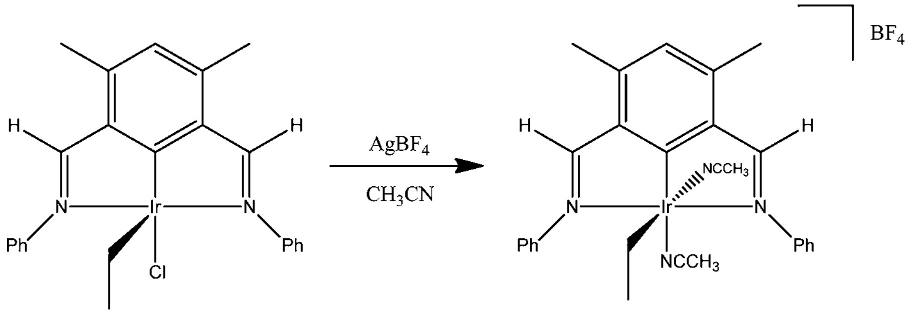

2 **7**

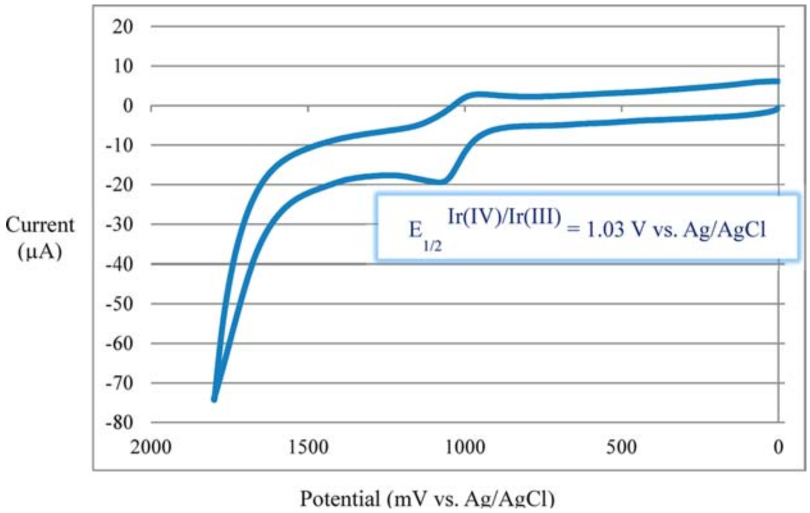

Figure 4. Cyclic voltammogram of **7** in acetonitrile at 50 mV/s.

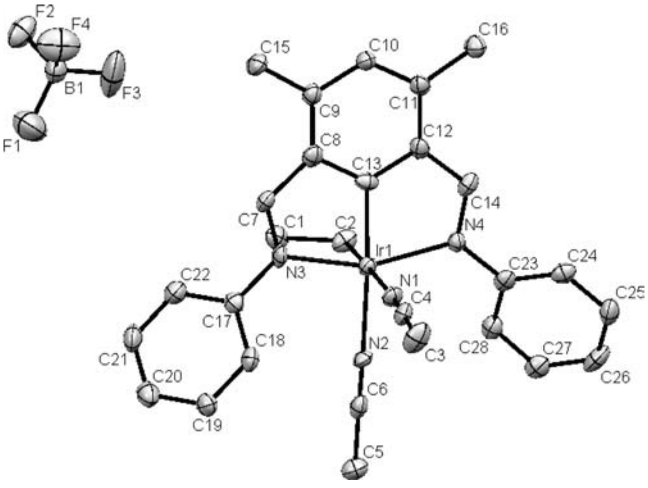

Figure 5. ORTEP of $[(NCN)Ir(CH_2CH_3)(NCCH_3)_2][BF_4]$ (**7**).

Table 4. Bond Lengths and Bond Angles of $[(NCN)Ir(CH_2CH_3)(NCCH_3)_2][BF_4]$ (7)

bond distances (Å)		bond angles (deg)	
Ir(1)−N(1)	2.132(4)	N(3)−Ir(1)−N(4)	157.90(168)
Ir(1)−N(2)	2.144(4)	N(3)−Ir(1)−C(13)	78.8(2)
Ir(1)−N(3)	2.065(4)	N(4)−Ir(1)−C(13)	79.2(2)
Ir(1)−N(4)	2.089(4)	C(13)−Ir(1)−C(2)	88.0(2)
Ir(1)−C(2)	2.096(5)	C(13)−Ir(1)−N(1)	94.96(19)
Ir(1)−C(13)	1.931(5)	C(13)−Ir(1)−N(2)	175.26(18)
		C(2)−Ir(1)−N(1)	176.87(18)
		C(2)−Ir(1)−N(2)	87.97(19)
		N(1)−Ir(1)−N(2)	89.17(17)

and this counter-intuitive C-13 assignment was verified by HMQC.

The five-coordinate, sixteen-electron Ir(III) complex **2** readily adds neutral two-electron donor ligands. Addition of water results in formation of the product $(NCN)Ir(CH_2CH_3)(Cl)(OH_2)$ (**3**) in which the weak σ-donating water ligand is trans to the aryl ligand of the NCN ligand (Scheme 4), indicating that the aryl group is a stronger trans donor than the ethyl group. The NCN ligand resonances shift only slightly in the proton NMR spectrum upon coordination of water, but the ethyl group signals shift more noticeably to 0.50 ppm for the $-CH_2$-protons and to −0.10 ppm for the $-CH_3$ protons. The coordinated water protons appear as a broad singlet at 4.82 ppm for this molecule.

Crystals of aquo complex **3** were grown from a solution of **3** in methylene chloride layered with hexanes at 277 K. The crystal structure of **3** shows tridentate coordination of the NCN ligand and a distorted octahedral geometry for the metal (Figure 1). The ethyl group is cis to the central aryl ring of the NCN ligand and the $-CH_3$ group of the ethyl is turned toward one of the imino nitrogens. The bound NCN ligand is planar with the exception of the imino phenyl rings, and they are twisted from the ligand plane by 51.9° and 49.3° in opposing directions. The Ir−C(10) (aryl sp^2 carbon) bond length is

Scheme 9. Synthetic Route to [(NCN)Ir(CH_2CH_3)(bpy)][BF_4]

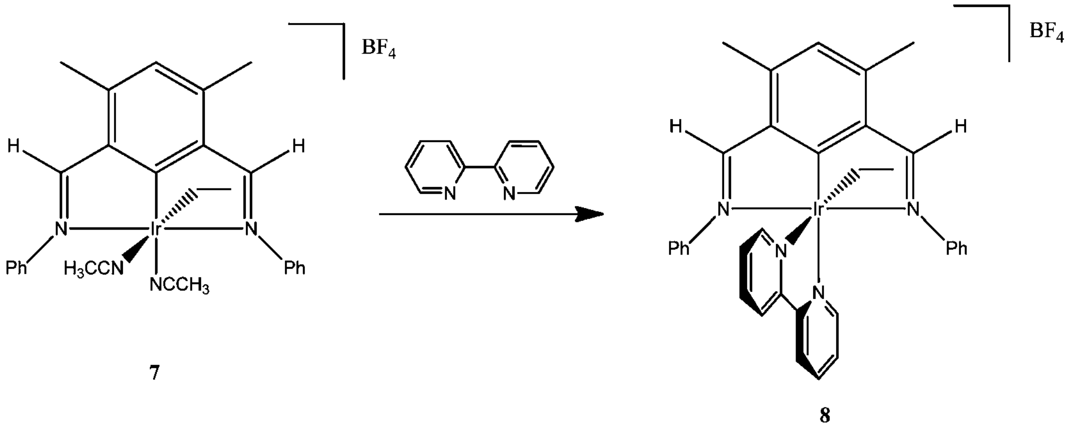

Scheme 10. Synthetic Route to [(NCN)Ir(CH_2CH_3)(OH_2)$_2$][BF_4] (9)

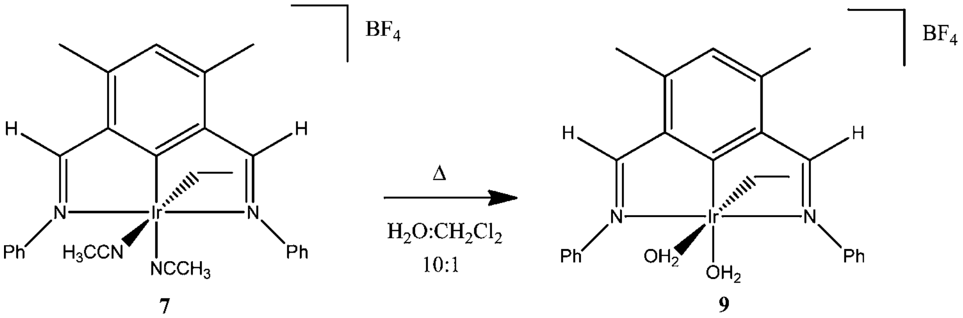

1.901 Å while the Ir−C(2) (ethyl sp^3 carbon) bond length is longer at 2.095 Å, a distance difference largely attributable to the difference in hybridization. The water ligand is trans to the aryl carbon, and the iridium−oxygen bond length is 2.259 Å, which is comparable to Ir−O bond lengths in other Ir−OH_2 complexes.[55−57] The iridium center sits below the N−N axis no doubt reflecting the directional orientation of the nitrogen donor lone pair electrons with a N(1)−Ir−N(2) bond angle of 159.35°. The N−Ir−C(10) angles are acute at 79.75° and 79.64° (Table 1).

Addition of triphenylphosphine results in formation of (NCN)Ir(CH_2CH_3)(Cl)(PPh_3) (**4**), in which the triphenylphosphine ligand is cis to the aryl moiety of the NCN ligand (Scheme 5). The two iminophenyl groups point downward, blocking the bulky triphenylphosphine ligand from occupying the site trans to the aryl ring. The strong sigma donation of the triphenylphosphine ligand together with the shielding effect of one of the aryl rings of the PPh_3 ligand (Figure 2) shifts the NCN ligand proton signals upfield from those of **2** in the ^1H NMR spectrum. The equivalent imino protons resonate at 8.42 ppm, compared to 8.82 ppm for the same protons in **2**, while the equivalent methyl groups appear at 2.44 ppm in **4** compared to the same moieties at 2.66 ppm in **2**. The ethyl group signals shift downfield to 1.43 and 0.00 ppm, and the $-CH_2-$ multiplet reflects three-bond coupling to phosphorus. The $^{31}P\{^1H\}$ NMR spectrum shows a single peak at −6.82 ppm for the bound phosphine.

Red crystals of **4** were grown by slow evaporation of a methylene chloride solution of **4** at room temperature. The crystal structure of **4** shows a distorted octahedral geometry (Figure 2). The NCN pincer ligand occupies three meridional sites as anticipated, and the weak field chloride ligand is located trans to the central aryl carbon. The ethyl group and the triphenylphosphine ligand are cis to the central aryl carbon and trans to one another. The steric bulk and stronger electron-donor properties of the triphenylphosphine ligand result in a slight elongation of the iridium−nitrogen bonds by 0.03 Å and the iridium-aryl carbon bond by 0.02 Å compared to the length of the analogous bonds in aquo adduct **3**. The iridium-ethyl carbon bond lengthens by 0.04 Å, and the iridium-chloride bond length is longer by 0.02 Å compared to **3**. The N−Ir−N bond angle is 157.76°, almost 2° smaller compared to the corresponding bond angle in **3** (Table 2).

Addition of trifluoromethanesulfonic acid to a methylene chloride solution of **2** results in formation of a dicationic chloride-bridged iridium dimer [(NCN)Ir(Cl)]$_2$[OTf]$_2$ (**5**) and loss of ethane (Scheme 6). The dimer does not react with silver salts. The ^1H and ^{13}C NMR spectra indicate a C_{2v} symmetric molecule. The four phenyl rings are equivalent, and the aromatic proton signals fall between 7.52 and 7.43 ppm; the four equivalent imino protons appear as a singlet at 8.48 ppm. The proton on the central aryl ring resonates at 7.00 ppm for both NCN ligands, and all four methyl groups are reflected in a singlet at 2.80 ppm.

Addition of a silver salt to complex **2** results in abstraction of the chloride ligand from the coordination sphere. Silver salts with coordinating counterions give neutral complexes; as an example, the reaction of **2** with silver acetate gives (NCN)Ir(CH_2CH_3)(OAc) (**6**) (Scheme 7). The ^1H NMR spectrum of **6** shows a C_s symmetric molecule. The imino protons are equivalent at 9.14 ppm, and the equivalent methyl groups from the NCN ligand appear at 2.64 ppm. The ethyl group appears as a quartet at 0.45 ppm ($-CH_2-$) and a triplet at 0.20 ppm

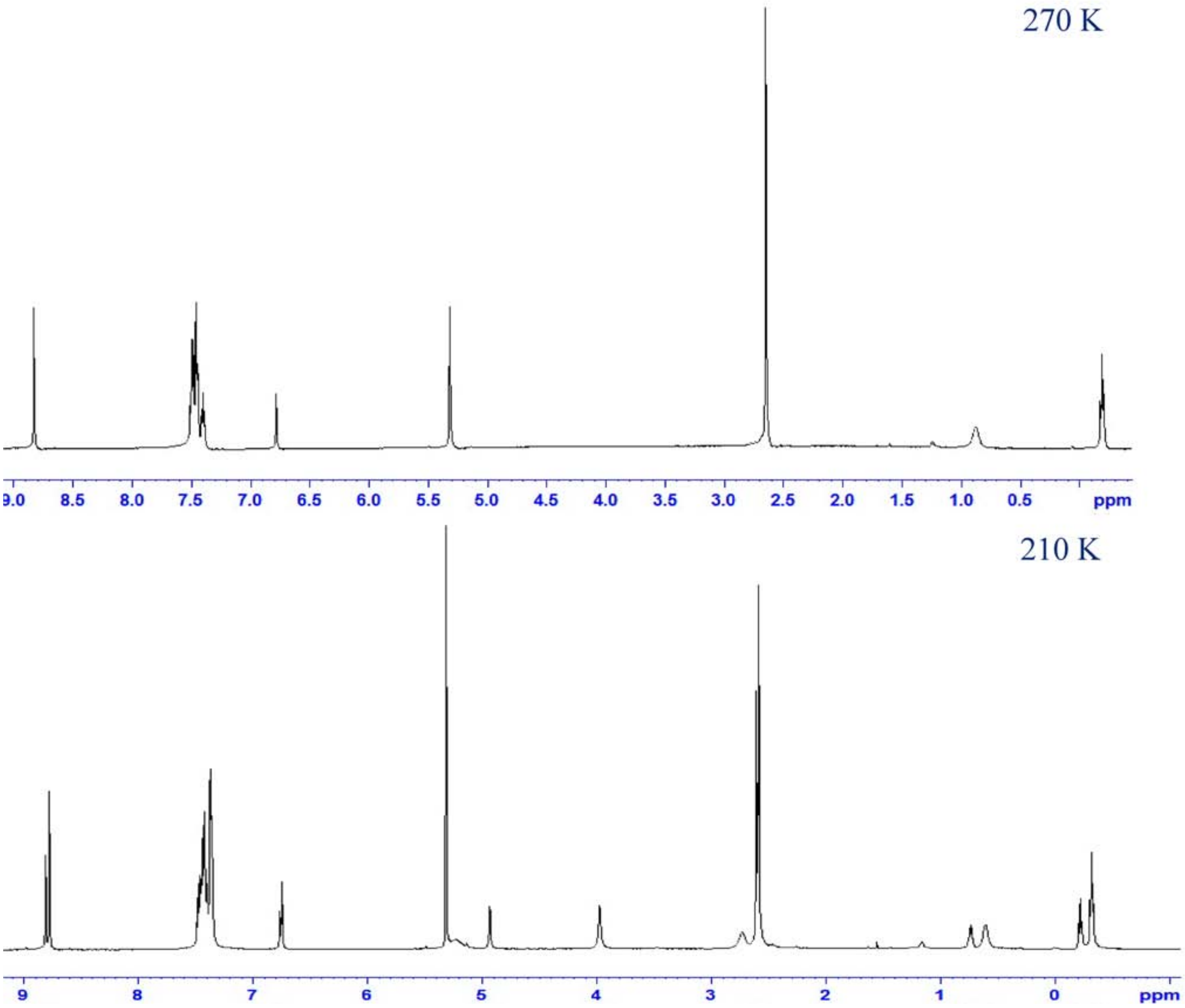

Figure 6. Variable temperature ^1H NMR spectrum of $[(NCN)Ir(Et)(OH_2)_2][OTf]$ (**9**).

Scheme 11. Ligand Exchange from 9

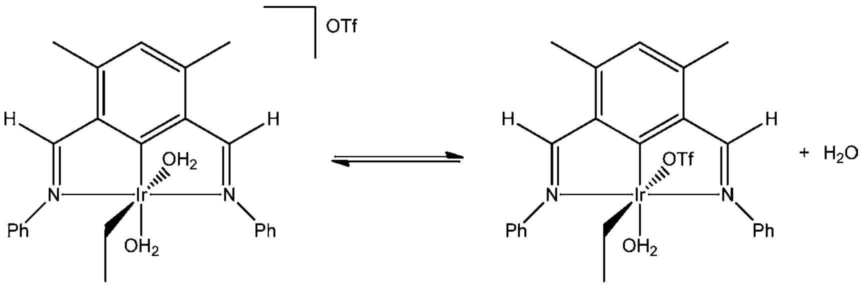

9

($-CH_3$). The methyl group of the acetate ligand gives rise to a singlet at 1.54 ppm.

Red crystals of acetate complex **6** were grown from an NMR tube sample of **6** in CD_2Cl_2 at 273 K. The crystal structure shows a distorted octahedral geometry, and again the NCN ligand occupies three meridional coordination sites (Figure 3). The planar acetate ligand is bound in a bidentate fashion through the two oxygen atoms. The plane of the acetate ligand is perpendicular to the plane of the NCN ligand. The Ir–N bond lengths are comparable to the other complexes reported here at 2.067 Å and 2.096 Å, as is the $Ir-C_{aryl}$ bond distance at 1.899 Å. The $Ir-C_{ethyl}$ bond length is slightly shorter at 2.070 Å compared to the analogous lengths in **3** and **4**. The ethyl group is located cis to the central aryl carbon with a C(12)–Ir–C(4) bond angle of 89.56°. The O(1)–Ir–O(2) bond angle is 57.86°, and the N(1)–Ir–N(2) bond angle is 158.64° (Table 3).

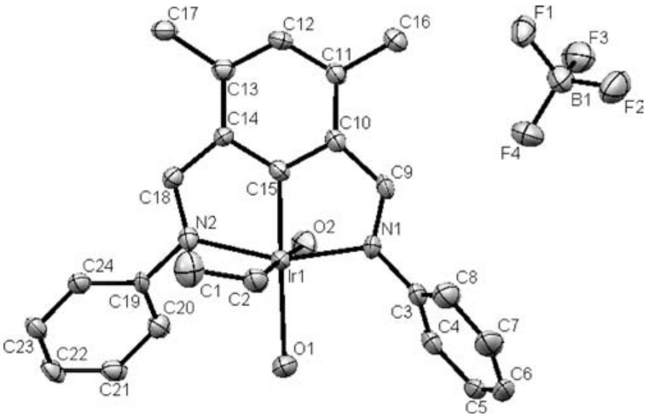

Figure 7. ORTEP of $[(NCN)Ir(CH_2CH_3)(OH_2)_2][BF_4]$ (**9**).

Table 5. Bond Lengths and Bond Angles of 9

bond distances (Å)		bond angles (deg)	
Ir(1)−N(1)	2.071(5)	N(1)−Ir(1)−N(2)	159.3(2)
Ir(1)−N(2)	2.056(5)	N(1)−Ir(1)−C(15)	79.6(2)
Ir(1)−O(1)	2.283(4)	N(2)−Ir(1)−C(15)	79.7(2)
Ir(1)−O(2)	2.254(5)	C(15)−Ir(1)−C(2)	92.3(3)
Ir(1)−C(2)	2.059(7)	C(15)−Ir(1)−O(1)	177.8(2)
Ir(1)−C(15)	1.896(6)	C(15)−Ir(1)−O(2)	91.8(2)
		C(2)−Ir(1)−O(1)	89.7(2)
		C(2)−Ir(1)−O(2)	175.4(2)
		O(1)−Ir(1)−O(2)	86.24(19)

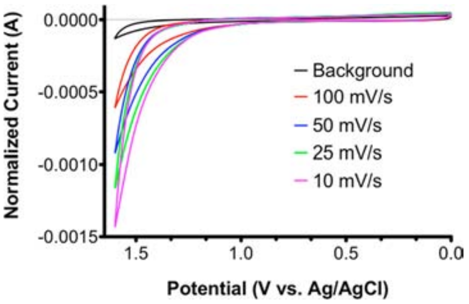

Figure 8. Cyclic voltammograms of **9** in 0.5 M phosphate buffer at pH = 2.15 with a glassy carbon working electrode at 298 ± 3 K.

Addition of excess silver tetrafluoroborate to **2** in acetonitrile results in abstraction of the chloride ligand and coordination of two acetonitrile ligands to iridium to give six-coordinate cationic $[(NCN)Ir(CH_2CH_3)(NCCH_3)_2][BF_4]$ (**7**) (Scheme 8). The acetonitrile ligands are cis to one another, and the ethyl ligand is cis to the central aryl carbon of the NCN ligand. The labile acetonitrile ligands in **7** provide convenient access to the Ir(III) center for adding poorly coordinating ligands or bidentate ligands.

The proton NMR spectrum of **7** indicates a C_s-symmetric complex. The acetonitrile ligands are inequivalent, with the two methyl resonances at 2.29 and 2.30 ppm, indicating that one is trans to the aryl ring while the other is trans to the ethyl group. The ethyl ligand appears as a quartet at 0.41 ppm and a triplet at 0.08 ppm. Cyclic voltammetry of **7** in acetonitrile shows a reversible wave at 1.03 V vs Ag/AgCl, and this one-electron redox process is assigned to the Ir(IV)/Ir(III) couple (Figure 4).

Red crystals of **7** were grown from slow diffusion of hexanes into a concentrated methylene chloride solution of **7** at 273 K. The crystal structure of **7** exhibits a distorted octahedral geometry where the planar NCN ligand occupies the expected three meridional coordination sites (Figure 5). The Ir−C_{aryl} bond length is 1.931 Å, while the Ir−C_{ethyl} bond length is 2.096 Å. The acetonitrile trans to the ethyl group has an Ir−N(1) bond distance of 2.132 Å while the acetonitrile trans to the aryl carbon has a Ir−N(2) bond distance of 2.144 Å. The N(3)−Ir−N(4) bond angle of the NCN ligand is 157.90° while the two acetonitrile ligand nitrogens are related by a N(1)−Ir−N(2) bond angle of 89.17° (Table 4).

Neutral bidentate ligands are readily coordinated to iridium by displacement of both acetonitrile ligands from **7**. Cationic $[Ir(III)(NCN)(CH_2CH_3)(bpy)][BF_4]$ (**8**) is formed within minutes upon addition of 1 equiv of bipyridine to a methylene chloride solution of **7** (Scheme 9).

The proton NMR spectrum of **8** shows a C_s-symmetric molecule. The imino protons (8.80 ppm) and the methyl groups (2.76 ppm) are equivalent. Since the bipyridine ligand lies on the mirror plane, the eight bipyridine protons are all inequivalent; they resonate in the range of 8.66 to 7.07 ppm. The ethyl group appears as a quartet at 1.05 ppm and a triplet at 0.27 ppm.

Addition of 30 mL of water to a concentrated 3 mL methylene chloride solution of the bis-acetonitrile complex **7**, followed by vigorous stirring for 12 h at 50 °C results in replacement of both acetonitrile ligands with aqua ligands to form $[(NCN)Ir(CH_2CH_3)(OH_2)_2][BF_4]$ (**9**) (Scheme 10). One aqua ligand is trans to the central aryl group of NCN while the other aqua ligand is trans to the ethyl group. Complex **9** is soluble in polar organic solvents as well as in water.

The proton NMR of **9** supports a C_s-symmetric complex with a mirror plane relating the two halves of the NCN ligand. The two imino protons are equivalent at 8.83 ppm, and the two methyl groups are equivalent at 2.66 ppm. The ethyl group appears as a quartet at 0.88 ppm and as a triplet at −0.18 ppm. All four aqua protons are represented by a broad peak at 2.20 ppm in CD_2Cl_2 because of rapid proton exchange. When the tetrafluoroborate counterion is replaced with a triflate counterion, the proton NMR shows two species at 210 K (Figure 6). One species is the cationic bis-aqua $[(NCN)Ir(CH_2CH_3)(OH_2)_2][OTf]$ while the second species is neutral and has triflate bound to iridium in place of the aqua ligand trans to the ethyl group, $(NCN)Ir(CH_2CH_3)(OH_2)(OTf)$ (Scheme 11). At room temperature, the ligand exchange between water and triflate is fast on the NMR time scale.

Red crystals of cationic bis-aqua complex **9** were grown by slow diffusion of hexanes into a concentrated methylene chloride solution of **9** at 273 K. The crystal structure shows a distorted octahedral geometry. The Ir−C_{aryl} bond length is 1.896 Å, and the Ir−C_{ethyl} bond length is 2.059 Å; both distances are the shortest of the observed structures (Figure 7). The two Ir−N bond distances are likewise short at 2.071 and 2.056 Å. The Ir−O(2) bond length is 2.254 Å while the Ir−O(1) bond length corresponding to the aqua ligand trans to the aryl ring is longer at 2.283 Å. The N(1)−Ir−N(2) bond angle is 159.3°, and the O(1)−Ir−O(2) bond angle is 86.24° (Table 5).

Cyclic voltammetric measurements were carried out at a glassy carbon working electrode with a Ag/AgCl (3 M NaCl) reference (measured at 0.207 V vs NHE) and platinum counter electrode in a phosphate buffered aqueous solution at pH = 2.15 with an ionic strength of 0.5 M. A cyclic voltammogram (CV) of **9** shows two oxidation waves at 1.05 and 1.28 V vs Ag/AgCl attributed to the Ir(IV)/Ir(III) couple and the Ir(V)/

Table 6. Crystal and Data Collection Parameters for (NCN)Ir(Et)(Cl)(OH_2) (3), (NCN)Ir(Et)(Cl)(PPh_3) (4), and (NCN)Ir(Et)(OAc) (6)

	3	4	6
empirical formula	$C_{24}H_{26}ClIrN_2O$	$C_{42}H_{39}ClIrN_2P$	$C_{26}H_{27}IrN_2O_2$
formula weight	586.12	830.37	591.70
color	red	red	red
temperature	100 K	100 K	100 K
crystal system	monoclinic	monoclinic	triclinic
space group	$P2_1/n$	$P2_1/n$	$P\bar{1}$
unit cell dimensions	a = 12.5082(3) Å	a = 11.7273(3) Å	a = 10.3583(2) Å
	b = 11.5034(3) Å	b = 16.9263(4) Å	b = 10.4763(2) Å
	c = 14.9983(4) Å	c = 17.7219(4) Å	c = 12.0455(3) Å
	α = 90.00°	α = 90.00°	α = 73.8230(10)°
	β = 93.8010(10)°	β = 95.4520(10)°	β = 83.5340(10)°
	γ = 90.00°	γ = 90.00°	γ = 62.6830(10)°
volume	2153.31(10) $Å^3$	3501.88(15) $Å^3$	1115.21(4) $Å^3$
Z	4	4	2
density (calculated)	1.808 mg/m^3	1.575 mg/m^3	1.762 mg/m^3
absorption coefficient	13.275 mm^{-1}	8.757 mm^{-1}	11.784 mm^{-1}
$F(000)$	1144.0	1656.0	580.0
crystal size	0.332 × 0.304 × 0.166 mm^3	0.35 × 0.1 × 0.079 mm^3	0.257 × 0.171 × 0.154 mm^3
θ range	9.7 to 147.42°	7.24 to 147.56°	7.64 to 133.14°
index ranges	$-15 \le h \le 15$	$-14 \le h \le 14$	$-12 \le h \le 11$
	$-14 \le k \le 13$	$-20 \le k \le 20$	$-12 \le k \le 12$
	$-18 \le l \le 18$	$-22 \le l \le 21$	$-14 \le l \le 14$
reflections collected	19808	33963	12793
data/restraints/parameters	4262/0/266	6959/0/427	3770/0/284
goodness-of-fit on F^2	1.234	1.048	1.183
final R indices [$I > 2\sigma(I)$] R indices (all data)	R1 = 0.0262,	R1 = 0.0235,	R1 = 0.0308,
	wR2 = 0.0671	wR2 = 0.0585	wR2 = 0.0725
	R1 = 0.0264,	R1 = 0.0260,	R1 = 0.0310,
	wR2 = 0.0672	wR2 = 0.0600	wR2 = 0.0727
largest diff. peak and hole	1.41 and −0.78 e $Å^{-3}$	1.13 and −0.74 e $Å^{-3}$	1.91 and −0.91 e $Å^{-3}$

Ir(IV) couple respectively (Figure 8). The potentials for these couples were derived from differential pulse voltammetry as the complex did not show a significant electrochemical response in the CV. This may be due to poor solubility of the Ir complex in the buffered aqueous medium or slow electron transfer between the complex and the electrode. Normalized CVs at scan rates of 10, 25, 50, and 100 mV/s show increasing normalized current with decreasing scan rates (Figure 8). The normalized current values were obtained by dividing the observed current by the square root of the scan rate as is appropriate for diffusion controlled redox couples. This is indicative of a catalytic process, although decomposition of the catalyst cannot be ruled out. The current remained constant (did not increase or decrease) over multiple scans.

SUMMARY

A nonheterocyclic bis(imino)aryl ligand with blocking methyl substituents, 4,6-dimethyl-1,3-benzenediphenylimine (NCHN), has been synthesized. Reaction with $[Ir(CH_2{=}CH_2)_2(Cl)]_2$ under mild conditions led to (NCN)Ir(CH_2CH_3)(Cl) via C−H activation at the central aryl position of the NCN ligand. This five-coordinate complex proved to be a versatile starting material for modification of the three remaining coordination sites. Neutral nucleophiles including water and triphenylphosphine could be readily added to the vacant sixth coordination site. Protonation of the ethyl group resulted in loss of ethane and formation of a dicationic chloride-bridged (NCN)Ir dimer. Alternatively, the chloride ligand could be abstracted from (NCN)Ir(CH_2CH_3)(Cl) to access various neutral and cationic species, including (NCN)Ir(CH_2CH_3)(OAc), [(NCN)Ir(CH_2CH_3)$(NCCH_3)_2$][BF_4], [(NCN)Ir(CH_2CH_3)(bpy)][BF_4], and [(NCN)Ir(CH_2CH_3)$(OH_2)_2$][BF_4].

EXPERIMENTAL SECTION

General Information. Unless otherwise noted, reactions were performed open to air. Methylene chloride, hexanes, pentane, diethyl ether, toluene, and tetrahydrofuran were purified by passage through an activated alumina column under a dry argon atmosphere. Methylene chloride-d_2 was dried over CaH_2 and degassed using standard freeze−pump−thaw techniques.

NMR spectra were recorded on Bruker DRX400, 500, 600 or AVANCE400 spectrometers. The electrochemical measurements were taken with a BAS100B electrochemical analyzer potentiostat. The electrodes were a planar BAS MF-2012 glassy carbon electrode, a platinum wire EG&G PARC K0266 counter electrode, and a Ag/AgCl EG&G PARC K0265 reference electrode.

Crystal and data collection parameters for **3**, **4**, and **6** are given in Table 6 and for **7** and **9** in Table 7.

4,6-Dimethyl-1,3-benzenediphenylimine (NCHN) (1). A 0.48 mL volume (5.34 mmol) of aniline was placed in a round-bottom flask with 0.50 g (2.67 mmol) of 4,6-dimethyl-1,3-benzenedicarboxaldehyde. A 0.015 g portion of (0.08 mmol) PTSA and 30 mL of toluene were added. The solution was refluxed for 24 h, then cooled to room temperature. The solvent was removed in vacuo, and methanol was added to precipitate the product. The 4,6-dimethyl-1,3-benzenediphenylimine was washed with methanol to give 0.70 g (2.0 mmol) of tan powder (78% yield). ^1H NMR ($CDCl_3$, δ): 8.75 (s, 2H, C*H*N) 8.66 (s, 1H, Ph C*H*), 7.42 (t, 4H, Ph C*H*), 7.26 (d, 2H, Ph C*H*), 7.24 (t, 4H, Ph C*H*), 7.15 (s, 1H, Ph C*H*), 2.65 (s, 6H, −C*H*$_3$). $^{13}C\{^1H\}$ NMR

Table 7. Crystal and Data Collection Parameters for [(NCN)Ir(Et)($NCCH_2$)$_2$][BF_4] (7) and [(NCN)Ir(Et)(OH_2)$_2$][BF_4] (9)

	7	9
empirical formula	$C_{28}H_{30}BF_4IrN_4$	$C_{24}H_{28}BF_4IrN_2O_2$
formula weight	701.57	655.49
color	orange	red
temperature	100 K	100 K
crystal system	triclinic	monoclinic
space group	$P\bar{1}$	$P2_1/c$
unit cell dimensions	a = 8.9633(2) Å	a = 26.0020(6) Å
	b = 11.9394(2) Å	b = 11.7258(3) Å
	c = 12.6935(2) Å	c = 16.4472(4) Å
	α = 82.3830(10)°	α = 90.00°
	β = 84.2520(10)°	β = 100.461(2)°
	γ = 85.7140(10)°	γ = 90.00°
volume	1337.05(4) $Å^3$	4931.3(2) $Å^3$
Z	2	8
density (calculated)	1.743 mg/m^3	1.766 mg/m^3
absorption coefficient	10.121 mm^{-1}	10.961 mm^{-1}
F(000)	688.0	2560.0
crystal size	0.224 × 0.095 × 0.026 mm^3	0.4 × 0.05 × 0.05 mm^3
θ range	7.48 to 133.2°	3.46 to 140.16°
index ranges	$-7 \leq h \leq 10$	$-31 \leq h \leq 31$
	$-14 \leq k \leq 14$	$-14 \leq k \leq 14$
	$-14 \leq l \leq 15$	$-19 \leq l \leq 20$
reflections collected	8056	28565
data/restraints/parameters	4431/0/348	9206/0/623
goodness-of-fit on F^2	1.078	1.038
final R indices [$I > 2\sigma(I)$] R indices (all data)	R1 = 0.0353,	R1 = 0.0409,
	wR2 = 0.0829	wR2 = 0.0960
	R1 = 0.0419,	R1 = 0.0538,
	wR2 = 0.0867	wR2 = 0.1036
largest diff. peak and hole	2.15 and −0.95e $Å^{-3}$	2.95 and −1.18 e $Å^{-3}$

($CDCl_3$, δ): 159.01 (CHN), 152.82 (Ph C), 141.47 (Ph C), 134.19 (Ph C), 132.73 (Ph C), 129.36 (Ph C), 126.01 (Ph C), 121.11 (Ph C), 19.96 (−CH_3). Analysis: Calculated: C, 84.58; H, 6.45; N, 8.97. Found: C, 84.55; H, 6.15; N, 8.75.

(NCN)Ir(CH_2CH_3)(Cl) (2). [Ir(C_2H_4)$_2$Cl]$_2$ (0.052 g, 0.092 mmol) was placed in a Schlenk flask under argon with 4,6-dimethyl-1,3-benzenediphenylimine (0.072 g, 0.23 mmol). Methylene chloride (20 mL) was added, and the mixture was stirred for 1 h. The solvent was removed in vacuo, and the dark red residue was run down an alumina column flushed with hexanes, methylene chloride, and eluted with methanol. Solvent was removed in vacuo, and the residue was triturated with hexanes to yield a dark red powder (0.13 g, 80%) . ^{1}H NMR (CD_2Cl_2, δ): 8.82 (s, 2H, C*H*N) 7.48 (m, 8H, imine Ph C*H*), 7.41 (t, 2H, imine Ph C*H*), 6.80 (s, 1H, Ph C*H*), 2.66 (s, 6H, Ph−C*H*$_3$), 0.96 (q, 2H, −C*H*$_2$−), −0.16 (t, 3H, −C*H*$_3$). ^{13}C{^{1}H} NMR (CD_2Cl_2, δ): 175.12 (CHN), 151.70, 141.05, 139.93, 130.00, 128.17, 124.08, 123.7 (Ph C), 19.74 (Ph-CH_3), 15.20 (−CH_2-), −12.87 (−CH_3). Analysis: Calculated: C, 50.74; H, 4.26; N, 4.93. Found: C, 50.57; H, 4.52; N, 5.04.

(NCN)Ir(CH_2CH_3)(Cl)(OH_2) (3). (NCN)Ir(Et)(Cl) (0.0086 g, 0.0015 mmol) was dissolved in CD_2Cl_2 (10 mL). Water (2 μL, 0.012 mmol) was added and mixed. The solvent was removed in vacuo, and the red residue was triturated with hexanes to give a orange powder (0.0084 g, 96% yield). ^{1}H NMR (CD_2Cl_2, δ, 293 K): 8.82 (s, 2H, C*H*N), 7.61 (d, 4H, *ortho*-C*H*), 7.45 (t, 4H, *meta*-C*H*), 7.35 (t, 2H, *para*-C*H*), 6.75 (s, 1H, Ar C*H*), 4.82 (broad s, 2H, Ir−O*H*$_2$), 2.65 (s, 6H, Ph−C*H*$_3$), 0.50 (q, 2H, −C*H*$_2$−), −0.10 (t, 3H, −C*H*$_3$). ^{13}C{^{1}H} NMR (CD_2Cl_2, δ, 293 K): 171.72 (CHN), 152.41, 139.79, 138.96, 129.63, 127.59, 123.97, 122.91 (Ar C), 19.60 (Ph-CH_3), 14.34 (−CH_2-), −6.19 (−CH_3). Analytical data: Calculated: C, 49.18; H, 4.62; N, 4.12. Found: C, 49.34; H, 4.47; N, 4.46.

(NCN)Ir(CH_2CH_3)(Cl)(PPh_3) (4). (NCN)Ir(Et)(Cl) (0.020 g, 0.035 mmol) was dissolved in CD_2Cl_2 (10 mL). Triphenylphosphine (0.0092 g, 0.035 mmol) was added and mixed, immediately resulting in a bright red solution. The solvent was removed in vacuo, and the orange-red residue was triturated with hexanes to give a bright orange powder (0.027 g, 0.033 mmol, 94% yield). ^{1}H NMR (CD_2Cl_2, δ, 295 K): 8.42 (s, 2H, C*H*N), 7.38, 7.34, 7.31, 7.03, 6.83 (m, 25H, Ph C*H*), 6.54 (s, 1H, Ar C*H*) 2.44 (s, 6H, Ph−C*H*$_3$), 1.43 (m, 2H, −C*H*$_2$−), 0.00 (q, 3H, −C*H*$_3$). ^{31}P{^{1}H} NMR (CD_2Cl_2, δ): −6.82 (s). ^{13}C{^{1}H} NMR (CD_2Cl_2, δ): 173.43 (CHN), 152.16, 140.88, 138.69, 133.69, 133.62, 132.40, 129.06, 128.96, 128.62, 127.65, 127.57, 125.64, 122.97 (Ph C), 19.66 (Ph-CH_3), 13.17 (−CH_2-), 2.22 (−CH_3). Analytical data: Calculated: C, 60.75; H, 4.73; N, 3.37. Found: C, 60.48; H, 4.60; N, 3.26.

[(NCN)Ir(Cl)]$_2$[OTf]$_2$ (5). (NCN)Ir(Et)(Cl) (0.016 g, 0.028 mmol) was dissolved in CH_2Cl_2 (10 mL), and trifluoromethanesulfonic acid (2.5 μL, 0.028 mmol) was added and mixed. The solvent was removed in vacuo and the orange-red residue was washed once with water to remove the excess acid. Then the residue was triturated with hexanes to give an orange powder (0.015 g, 80% yield). ^{1}H NMR (CD_2Cl_2, δ, 293 K): 8.48 (s, 2H, C*H*N) 7.52 (m, 8H, imine Ph C*H*), 7.43 (m, 2H, imine Ph C*H*), 7.00 (s, 1H, Ph C*H*), 2.80 (s, 6H, Ph−C*H*$_3$). ^{13}C{^{1}H} NMR (CD_2Cl_2, δ, 293 K): 180.84 (CHN), 150.41, 144.27, 140.24, 130.19, 129.06, 126.68, 123.11, 120.12 (Ph C), 19.38 (Ph-CH_3). Analytical data: Calculated: C, 40.14; H, 2.78; N, 4.07. Found: C, 40.15; H, 3.20; N, 3.64.

(NCN)Ir(CH_2CH_3)(OAc) (6). (NCN)Ir(Et)(Cl) (0.020 g, 0.035 mmol) was dissolved in CH_2Cl_2 (10 mL), and excess silver acetate (0.10 g, 0.60 mmol) was added and stirred for 1 h. The mixture was filtered, and the solvent was removed in vacuo, followed by a hexanes wash to produce a red powder (0.018 g, 0.030 mmol, 87% yield). ^{1}H NMR (CD_2Cl_2, δ, 289 K): 9.14 (s, 2H, C*H*N), 7.51 (d, 4H, *ortho*-Ph C*H*), 7.46 (t, 4H, *meta*-Ph C*H*), 7.37 (t, 2H, *para*-Ph C*H*), 6.73 (s, 1H, Ar C*H*), 2.64 (s, 6H, Ph−C*H*$_3$), 1.54 (s, 3H, OAc), 0.45 (q, 2H, −C*H*$_2$−), 0.20 (t, 3H, −C*H*$_3$). ^{13}C{^{1}H} NMR ($CDCl_3$, δ): 171.24 (CHN), 151.57, 139.71, 139.29, 129.32, 127.50, 123.93, 122.72 (Ph C), 68.34 (OAc-C), 25.24 (OAc-CH_3), 19.75 (Ph-CH_3), 14.78 (−CH_2-), −7.86 (−CH_3). Analytical data: Calculated: C, 52.77; H, 4.60; N, 4.73. Found: C, 52.32; H, 4.77; N, 5.10.

[(NCN)Ir(CH_2CH_3)($NCCH_3$)$_2$][BF_4] (7). (NCN)Ir(CH_2CH_3)(Cl) (0.20 g, 0.35 mmol) was placed in a Schlenk flask and dissolved in acetonitrile (10 mL). Silver tetrafluoroborate (0.23 g, 1.2 mmol) was added, and the mixture was stirred 1 h. The solution was filtered, and the solvent was removed in vacuo. The residue was dissolved in a minimum amount of methylene chloride and placed on a silica plug. Hexanes and methylene chloride washed the complex, and it was eluted with ethyl acetate (0.24 g, 0.34 mmol, 98% yield). ^{1}H NMR (CD_2Cl_2, δ, 293 K): 8.71 (s, 2H, C*H*N) 7.54 (t, 4H, *meta*-Ph C*H*), 7.43 (d, 4H, *ortho*-Ph C*H*), 7.41 (t, 2H, *para*-Ph C*H*), 6.82 (s, 1H, Ph C*H*), 2.66 (s, 6H, Ph−C*H*$_3$), 2.25, 2.23 (each a s, each 3H, NCC*H*$_3$), 0.41 (q, 2H, −C*H*$_2$−), 0.08 (t, 3H, −C*H*$_3$). ^{13}C{^{1}H} NMR (CD_2Cl_2, δ): 175.05 (CHN), 151.17, 141.61, 139.98, 129.72, 128.34, 123.91, 119.38, 117.06 (Ph C), 19.60 (Ph-CH_3), 15.30 (−CH_2-), 3.46, 3.30 ($NCCH_3$), −8.71 (−CH_3). Analytical data: Calculated: C, 47.97; H, 4.31; N, 7.99. Found: C, 47.72; H, 4.37; N, 7.71.

[(NCN)Ir(CH_2CH_3)(bpy)][OTf] (8). [(NCN)Ir(Et)($NCCH_3$)$_2$]-[OTf] (0.020 g, 0.029 mmol) was placed in a round-bottom flask and dissolved in CH_2Cl_2. Bipyridine (0.0045 g, 0.029 mmol) was added. The mixture was stirred for 5 min, and the solvent was removed in vacuo. The resulting bright red residue was washed with hexanes to produce a bright red powder (0.021 g, 0.027 mmol, 93% yield). ^{1}H NMR (CD_2Cl_2, δ, 295 K): 8.80 (s, 2H, C*H*N), 8.66 (d, 1H, bpy C*H*), 8.37 (d, 1H, bpy C*H*), 8.19 (t, 1H, bpy C*H*), 7.97 (m, 3H, bpy C*H* and Ph C*H*), 7.56 (t, 1H, bpy C*H*), 7.45 (t, 1H, bpy C*H*), 7.34 (t, 1H, bpy C*H*), 7.07 (t, 1H, bpy C*H*), 7.00 (s, 1H, Ph C*H*), 6.99 (t, 4H, Ph C*H*), 6.46 (d, 4H, Ph C*H*) 2.76 (s, 6H, Ph−C*H*$_3$), 1.05 (q, 2H, −C*H*$_2$−), 0.27 (t, 3H, −C*H*$_3$). ^{13}C{^{1}H} NMR ($CDCl_3$, δ): 173.94

(CHN), 151.75, 141.16, 139.99, 129.65, 127.83, 124.32, 123.72, 121.54 (Ph C), 19.76 (Ph-CH_3), 15.17 (−CH_2-), −12.66 (−CH_3). Analytical data: Calculated: C, 50.17; H, 3.85; N, 6.69. Found: C, 50.07; H, 3.97; N, 7.30.

$[(NCN)Ir(CH_2CH_3)(OH_2)_2][BF_4]$ (9). $[(NCN)Ir(CH_2CH_3)(NCCH_3)_2][BF_4]$ (0.10 g, 0.143 mmol) was dissolved in methylene chloride (3 mL) in a round-bottom flask open to the atmosphere. Thirty milliliters of deionized water was added, and the mixture was heated to 50 °C while stirring vigorously for 18 h. The mixture was filtered, and the solvent was removed in vacuo and the dark red residue was triturated with hexanes to give a dark red powder (0.076 g, 0.116 mmol, 81% yield). ^{1}H NMR (CD_2Cl_2, δ, 295 K): 8.83 (s, 2H, C*H*N) 7.47 (m, 8H, imine Ph C*H*), 7.41 (t, 2H, imine Ph C*H*), 6.79 (s, 1H, Ph C*H*), 2.66 (s, 6H, Ph−CH_3), 2.2 (broad s, 4H, OH_2), 0.88 (q, 2H, −CH_2−), −0.18 (t, 3H, −CH_3). $^{13}C\{^1H\}$ NMR (CD_2Cl_2, δ): 175.12 (CHN), 151.75, 141.16, 139.99, 129.65, 127.83, 124.32, 123.72, 121.54 (Ph C), 19.76 (Ph-CH_3), 15.17 (−CH_2-), −12.66 (−CH_3). Analytical data: Calculated: C, 43.97; H, 4.31; N, 4.27. Found: C, 44.36; H, 4.18; N, 4.24.

ASSOCIATED CONTENT

Supporting Information

Crystallographic data in CIF format and representative ^{1}H NMR spectra. This material is available free of charge via the Internet at http://pubs.acs.org.

AUTHOR INFORMATION

Corresponding Author

*E-mail: leah.a.wingard@gmail.com.

Notes

The authors declare no competing financial interest.

ACKNOWLEDGMENTS

This material is based upon work wholly supported as part of the UNC EFRC, Center for Solar Fuels, an Energy Frontier Research Center funded by the U.S. Department of Energy, Office of Science, Office of Basic Energy Sciences under Award Number DE-SC0001011.

REFERENCES

(1) Benito-Garagorri, D.; Kirchner, K. *Acc. Chem. Res.* **2008**, *41*, 201.

(2) Nelson, S. M.; Dahlhoff, W. V. *J. Chem. Soc.* **1971**, *13*, 2184.

(3) Moulton, C. J.; Shaw, B. L. *J. Chem. Soc., Dalton Trans.* **1976**, 1020.

(4) van Koten, G.; Timmer, K.; Noltes, J. G.; Spek, A. L. *J. Chem. Soc., Chem. Commun.* **1978**, 250.

(5) Creaser, C. S.; Kaska, W. C. *Inorg. Chim. Acta* **1978**, *30*, L325.

(6) Rimml, H.; Venanzi, L. M. *J. Organomet. Chem.* **1883**, *259*, C6.

(7) van Koten, G. *Pure Appl. Chem.* **1989**, *61*, 1681.

(8) Choi, J.; MacArthur, A. H. R.; Brookhart, M.; Goldman, A. S. *Chem. Rev.* **2011**, *111*, 1761.

(9) Albrecht, M.; van Koten, G. *Angew. Chem., Int. Ed.* **2001**, *40*, 3750.

(10) Singleton, J. T. *Tetrahedron* **2003**, *59*, 1837.

(11) van der Ploeg, A. F. M. J.; van Koten, G.; Brevard, C. *Inorg. Chem.* **1982**, *21*, 2878.

(12) Albrecht, M.; Gossage, R. A.; Lutz, M.; Spek, A. L.; van Koten, G. *Chem.—Eur. J.* **2000**, *6*, 1431.

(13) Albrecht, M.; Schlupp, M.; Bargon, J.; van Koten, G. *Chem. Commun.* **2001**, 1874.

(14) van der Boom, M. E.; Milstein, D. *Chem. Rev.* **2003**, *103*, 1759.

(15) Kang, P.; Cheng, C.; Chen, Z.; Schauer, C. K.; Meyer, T. J.; Brookhart, M. *J. Am. Chem. Soc.* **2012**, *134*, 5500.

(16) Lee, D. W.; Jensen, C. M.; Morales-Morales, D. *Organometallics* **2003**, *22*, 4744.

(17) Bernskoetter, W. H.; Hanson, S. K.; Buzak, S. K.; Davis, Z.; White, P. S.; Swartz, R.; Goldberg, K. I.; Brookhart, M. *J. Am. Chem. Soc.* **2009**, *131*, 8603.

(18) Mohammad, H. A. Y.; Grimm, J. C.; Eichele, K.; Mack, H.; Speiser, B.; Novak, F.; Quintanilla, M. G.; Kaska, W. C.; Mayer, H. A. *Organometallics* **2002**, *21*, 5775.

(19) Winter, A. M.; Eichele, K.; Mack, H.; Kaska, W. C.; Mayer, H. A. *Organometallics* **2005**, *24*, 1837.

(20) Zhang, X.; Kanzelberger, M.; Emge, T. J.; Goldman, A. S. *J. Am. Chem. Soc.* **2004**, *126*, 13192.

(21) Choi, J.; Choliy, Y.; Zhang, X.; Emge, T. J.; Krogh-Jespersen, K.; Goldman, A. S. *J. Am. Chem. Soc.* **2009**, *131*, 15627.

(22) Bailey, B. C.; Schrock, R. R.; Kundu, S.; Goldman, A. S.; Huang, Z.; Brookhart, M. *Organometallics* **2009**, *28*, 355.

(23) Goldman, A. S.; Roy, A. H.; Huang, Z.; Ahuja, R.; Schinski, W.; Brookhart, M. *Science* **2006**, *312*, 257.

(24) Goettker-Schnetmann, I.; Brookhart, M. *J. Am. Chem. Soc.* **2004**, *126*, 9330.

(25) Goettker-Schnetmann, I.; White, P. S.; Brookhart, M. *Organometallics* **2004**, *23*, 1766.

(26) Kundu, S.; Choliy, Y.; Zhuo, G.; Ahuja, R.; Emge, T. J.; Warmuth, R.; Brookhart, M.; Krogh-Jespersen, K.; Goldman, A. S. *Organometallics* **2009**, *28*, 5432.

(27) Gupta, M.; Hagen, C.; Flesher, R. J.; Kaska, W. C.; Jensen, C. M. *Chem. Commun.* **1996**, *17*, 2083.

(28) Gupta, M.; Hagen, C.; Kaska, W. C.; Cramer, R. E.; Jensen, C. M. *J. Am. Chem. Soc.* **1997**, *119*, 840.

(29) Lee, D. W.; Kaska, W. C.; Jensen, C. M. *Organometallics* **1998**, *17*, 1.

(30) Bernskoetter, W. H.; Brookhart, M. *Organometallics* **2008**, *27*, 2036.

(31) Morales-Morales, D.; Cramer, R. E.; Jensen, C. M. *J. Organomet. Chem.* **2002**, *654*, 44.

(32) Morales-Morales, D.; Redon, R.; Yung, C.; Jensen, C. M. *Inorg. Chim. Acta* **2004**, *357*, 2953.

(33) Liu, F.; Goldman, A. S. *Chem. Commun.* **1999**, *7*, 655.

(34) Renkema, K. B.; Kissin, Y. V.; Goldman, A. S. *J. Am. Chem. Soc.* **2003**, *125*, 7770.

(35) Zhu, K.; Achord, P. D.; Zhang, X.; Krogh-Jespersen, K.; Goldman, A. S. *J. Am. Chem. Soc.* **2004**, *126*, 13044.

(36) Punji, B.; Emge, T. J.; Goldman, A. S. *Organometallics* **2010**, *29*, 2702.

(37) Jensen, C. M. *Chem. Commun.* **1999**, *24*, 2443.

(38) Yang, J.; White, P. S.; Brookhart, M. *J. Am. Chem. Soc.* **2008**, *130*, 17509.

(39) Findlater, M.; Schultz, K. M.; Bernskoetter, W. H.; Cartwright-Sykes, A.; Heinekey, D. M.; Brookhart, M. *Inorg. Chem.* **2012**, *51*, 4672.

(40) Lee, D. H.; Hong, S. J.; Park, S. *Bull. Korean Chem. Soc.* **2008**, *29*, 187.

(41) Fossey, J. S.; Richards, C. J. *Organometallics* **2002**, *21*, 5259.

(42) Balamurugan, R.; Palaniandavar, M.; Halcrow, M. A. *Polyhedron* **2006**, *25*, 1077.

(43) Vila, J. M.; Gayoso, M.; Pereira, T.; Torres, M. L.; Fernandez, J. J.; Fernandez, A.; Ortigueira, J. M. *J. Organomet. Chem.* **1996**, *506*, 165.

(44) Simon, P.; de Proft, F.; Jambor, R.; Ruzicka, A.; Dostal, L. A. *Angew. Chem., Int. Ed.* **2010**, *49*, 1.

(45) Wilkinson, A. J.; Goeta, A. E.; Foster, C. E.; Williams, J. A. G. *Inorg. Chem.* **2004**, *43*, 6513.

(46) Whittle, V. L.; Williams, J. A. G. *Inorg. Chem.* **2008**, *47*, 6596.

(47) Yutaka, T.; Obara, S.; Ogawa, S.; Mozaki, K.; Ikeda, N.; Ohno, T.; Ishii, Y.; Sakai, K.; Haga, M. *Inorg. Chem.* **2005**, *44*, 4767.

(48) Ashizawa, M.; Yang, L.; Kobayashi, K.; Sato, H.; Yamagishi, A.; Okuda, F.; Harada, T.; Kuroda, R.; Haga, M. *Dalton Trans.* **2009**, *10*, 1700.

(49) Ito, J.; Shiomi, T.; Mishiyama, H. *Adv. Synth. Catal.* **1988**, *348*, 1235.

(50) Oakley, S. H.; Coogan, M. P.; Arthur, R. J. *Organometallics* **2007**, *26*, 2285.

(51) Bonifacio, M. C.; Robertson, C. R.; Jung, J.; King, D. *J. Org. Chem.* **2005**, *70*, 8552.
(52) Rehahn, M.; Schluter, A.; Feast, W. J. *Synthesis* **1988**, *5*, 386.
(53) Pelascini, F.; Peruch, F.; Lutz, P. J.; Wesolek, M.; Kress, J. *Eur. Polym. J.* **2005**, *41*, 1288.
(54) Onderdelinden, A. L.; van der Ent, A. *Inorg. Chim. Acta* **1972**, *6*, 420.
(55) Schley, N. D.; Blakemore, J. D.; Subbaiyan, N. K.; Incarvtio, C. D.; D'Souza, F.; Crabtree, R. H.; Brudvig, G. W. *J. Am. Chem. Soc.* **2011**, *133*, 10473.
(56) Kanemitsu, H.; Harada, R.; Ogo, S. *Chem. Commun.* **2010**, *46*, 3083.
(57) Hughes, R. P.; Lindner, D. C.; Smith, J. M.; Zhang, D.; Incarvito, C. D.; Lam, K.; Liable-Sands, L. M.; Sommer, R. D.; Rheingold, A. L. *J. Chem. Soc., Dalton Trans.* **2001**, 2270.